Available online at www.sciencedirect.com
ScienceDirect
Solar Energy 84 (2010) 215–226
SOLAR ENERGY
www.elsevier.com/locate/solener

Satellite-based snow identification and its impact on monitoring photovoltaic systems

Georg Wirth [a,*], Marion Schroedter-Homscheidt [b], Mike Zehner [a], Gerd Becker [a]

[a] University of Applied Sciences – Munich, Department of Electrical Engineering, Solar Technology Laboratory, Lothstrasse. 64, 80323 Munich, Germany
[b] German Aerospace Center (DLR), German Remote Sensing Data Center (DFD), Oberpfaffenhofen, P.O. Box 1116, 82234 Wessling, Germany

Received 17 September 2008; received in revised form 15 October 2009; accepted 29 October 2009
Available online 24 December 2009

Communicated by: Associate Editor David Renne

Abstract

Earth observation allows the separation of snow cover and cloudiness using multispectral measurements. Several satellite-based snow monitoring services are available, ranging from regional to world-wide scales. Using these data enables photovoltaic (PV) plant management to differentiate between failures due to snow coverage on a PV system and other error sources. Additionally, yield estimates for solar siting are improved. This paper presents a validation study from January to April 2006 comparing satellite-based datasets with ground measurements from German and Swiss meteorological stations. A false alarm rate, an error due to irradiance underestimation, the availability of daily data, and the classification accuracy are introduced as quality metrics. Compared to Switzerland, generally a higher accuracy is found in all datasets for Southern Germany. The most significant difference among the datasets is found in the error pattern shifting from too much snow (which results in an error due to underestimation of irradiance) to too little snow detection, causing a false alarm in PV monitoring.

Overall, the data records of the Land Surface Analysis Satellite Application Facility (LSA SAF), the German Aerospace Center (DLR) and the Interactive Multisensor Snow and Ice Mapping System (IMS) are found to be most suitable for solar energy purposes. The IMS dataset has a low false alarm rate (4%) and a good data availability (100%) making it a good choice for power plant monitoring, but the error due to underestimation relevant in site auditing is large with 59%. If a cumulative snow cover algorithm is applied to achieve information every day as needed both for power plant monitoring and site auditing, both the DLR and the LSA SAF datasets are comparable with classification accuracies of 70%, false alarm rates of 37% and 34%, respectively, and errors due to irradiance underestimation in 26% and 27% of all coincidences.

Keywords: Snow cover; Satellite-derived snow monitoring; Automatic failure detection; Photovoltaic system; Monitoring

1. Introduction

A higher percentage of fluctuating renewable energy such as solar energy in the power grid creates new challenges for the grid management. Monitoring capabilities have to be improved so that performance data are easy to access, especially for the large number of small grid-connected photovoltaic (PV) systems.

A PV monitoring system observes electrical power data as well as environmental parameters such as global radiation and surrounding air temperature. Each panel can be described as a mathematic model with electrical power as an output parameter. Taking the whole PV power plant into consideration, an efficiency factor chain can be built, reaching from global irradiation to the panels, to the system's characteristic losses, to the inversion, and, finally, to the power delivered into the grid. Using this model and characteristic data for the specific PV system allows one to compute the theoretical power output for a given

* Corresponding author. Tel.: +49 89 1265 3478.
E-mail address: georg.wirth@hm.edu (G. Wirth).

0038-092X/$ - see front matter © 2009 Elsevier Ltd. All rights reserved.
doi:10.1016/j.solener.2009.10.023

irradiation. Serious plant failures may be determined by comparing an estimate with the actual power output. A power plant's defect can be detected if the two datasets become unequal over time.

The basis for proper estimates is a reliable input dataset – either from on-site or satellite measurement – while incorrect input data might cause a false alarm. A typical false alarm situation is often observed if snow-covered PV panels deliver only a small energy yield while the estimated output is high based on high global radiation correctly identified by on-site or satellite measurements. This is only a temporary problem without causing a maintenance demand, since the plant will be fully operational again after the melting. Using additional information on snow coverage from external information sources could reduce the false alarm rate.

Satellite-based monitoring systems rely on irradiance data derived from a meteorological satellite. They are replacing on-site measurements with a reference cell or a pyranometer to determine the estimated energy yield of a PV system (Drews, 2007). Earth observation also allows the detection of snow cover and the discrimination of clouds from snow in different spatial scales. Instead of indicating snow cover on the basis of locally measured temperature and radiation parameters only, the monitoring system can also access several satellite-based snow cover services available and ranging from regional to world-wide scales.

The most significant problem is snow on the panels as described above. Another problem occurs if a cloud is interpreted as snow in the satellite radiation retrieval. This case results in a low yield estimated by the satellite while the plant has a high yield indeed. In such cases, other possible errors in the plant will not be detected and the analysis of historical data sets would result in a yield underestimation.

Most of the satellite-based datasets are designed for global use and large-scale monitoring of the atmospheric energy and water balance. Validation studies typically target water resource monitoring, hydrologic modeling, and climate change assessment (Brubaker and Tarpley, 2005) and often focus on northern, sparely populated and often forested areas (Hall et al., 1998, 2004). Typically, these studies are based on 8-day composite snow maps (Hall et al., 2002a), while photovoltaic plant monitoring relies on near-real-time datasets. There are also studies available in Northern America with a similar focus (Romanov et al., 2000; Simic et al., 2004; Bitner et al., 2002; Maurer et al., 2003). Romanov et al. (2000) compare automated snow cover monitoring with Geostationary Operational Environmental Satellite (GOES), Special Sensor Microwave/Imager (SSM/I) and Interactive Multisensor Snow and Ice Mapping System (IMS) data against ground observations. All products reach over 80% classification accuracy in the Northern US. Simic et al. (2004) find classification accuracies above 80% for the GOES, SSM/I combination and the Moderate-resolution Imaging Spectroradiometer (MODIS) snow cover product in Canada. Bitner et al. (2002) compare National Oceanic and Atmospheric Administration (NESDIS), National Operational Hydrologic Remote Sensing Center (NOHRSC) and MODIS data finding that all three are comparable in their results. Maurer et al. (2003) evaluate the MODIS product against the background of stream flow prediction, and state its ability to map snow in forest regions. Apart from Romanov et al. (2000), these studies do generally not separate between over- and underestimation of snow cover as needed in a validation suitable for solar energy. Other meteorological validation studies intercompare different satellite based earth observation technologies in terms of area based percentages (e.g. Basist et al., 1996) but do not state the correspondence to certain coordinates.

Chapter 2 describes possible error sources in snowy conditions from the point of view of solar energy plant monitoring and introduces appropriate quality metrics. Chapter 3 provides an overview of existing satellite-based services offering snow cover information. Chapter 4 shows the results of a validation study divided into three different scenarios. First, all datasets are used as supplied by the provider and evaluated for every day in the given period. Second, only clear-sky cases are evaluated, as they are most relevant with low cloud cover and high radiation. Third, a cumulative algorithm is applied to interpolate those datasets with information gaps on days with cloud cover. Finally, chapter 5 concludes this paper.

2. Methods

2.1. Error sources in snow conditions

When comparing snow cover information derived from satellites with the actual snow cover, several more or less relevant faults can be observed. There are three possible conditions measured by the satellite: cloudless, cloudless with snow cover, and cloudless without snow cover. In contrast, only two conditions are observed on the ground: snow and snow-free. In a first approach, only four possibilities are taken into consideration: snow/snow-free as seen by the satellite and snow/snow-free as indicated by the ground measurement. There are two correct classifications, i.e., A and E and two incorrect cases, i.e., B and D (Table 1).

2.1.1. Case A

If an existing snow cover is identified correctly in the satellite pixel, the plant management system will calculate a low yield matching the actual power output of the plant. A site audit will estimate the yield correctly.

2.1.2. Case E

In this case, snow is neither located on the module, nor in the pixel. There is no influence on the plant management or site auditing; the full yield can be estimated.

2.1.3. Case B

Most relevant is the occurrence of snow cover without a correct detection. Satellite irradiance measurements would normally show high solar yield estimates; the yield

Table 1
Error sources for photovoltaic plant monitoring in snow conditions.

Gound conditions		Satellite measurement Snow in picture element	No snow in picture element	Missing/cloud
		Case A	Case B	Case C
	Conditions	Correct information	Underestimation of snow cover	Snow is interpreted as clouds or clouds above snow are identified correctly
Snow on panel	Effect on irradiance calculation	Satellite displays low yield plant has low yield	Satellite displays high yield plant has low yield	Satellite displays low yield due to cloudiness plant has low yield due to snow and possibly clouds
		Case D	Case E	Case F
	Conditions	Too much snow displayed cloud is interpreted as snow	Correct information	Normal operation cloud is detected correctly
Clear of snow on ground	Effect on irradiance calculation	Satellite displays low yield plant has high yield possible error in the plant will not be detected	Satellite displays high yield plant has high yield	Satellite displays low yield due to cloudiness plant has low yield due to clouds

observed is, however, very small due to snow cover on the panels. The plant management system interprets this as the plant's fault and generates an alarm engaging the maintenance team for an onsite check, even though there is only snow on the modules. This would also be the case without auxiliary snow detection, but now the problem is even more serious, since snow – as this cause of an error – is supposed to be eliminated. In a yield estimate, such error cases increase a power plant's amortization period, leading to losses for both operator and investor. An investment decision might thus be made in favor of the wrong location, and due to snow cover, a lower profit will be made than at the optimal location.

2.1.4. Case D

The satellite dataset indicates a snow cover, though none exists, leading the monitoring system to observe a higher yield than estimated. In site audits, this causes an error due to underestimation of solar energy yield. For yield estimations, any variation – regardless whether positive or negative – is problematic. In monitoring schemes, no alarm will be created, as this is not an indicator for a fault in the plant. Therefore, this case is not as important for plant monitoring as case B. Nevertheless, the sensibility decreases because a potential system error would be indicated as a loss caused by snow and not detected early enough.

Looking closer at the topic, visibility of the ground by the satellite needs to be introduced additionally. If the satellite detects a cloud, no data on the situation on the ground are available. Some data providers set such pixels to "Missing"/"Cloud", but not all datasets contain this information. This leads to two more cases: C and F.

2.1.5. Case C

If there is snow on the ground and the satellite indexes a cloud cover, there are two possibilities: either snow has been confused with a cloud, or a cloud over snow has been indexed correctly. This is neither critical in the management system nor in the yield estimates because regardless of whether the plant's observed power output will be low due to snow or low due to cloud cover, the estimated output will be correctly indicated as low.

2.1.6. Case F

The case with no snow on the ground and the satellite indexing a cloud is also unproblematic. This means that a cloud cover has been indexed correctly and both observed output and estimated output are low. Please note that the frequent case of an erroneously indexed cloud over snow-free surfaces is not treated in this snow-specific validation study.

Generally, snow can be recognized as "on the panels" or "on the ground". Snow on the panel, but not on the ground, is only a transition state not taken into consideration in this study. With a low air temperature, but relatively high ground temperature, the freshly fallen snow stays on the panel, yet melts on the ground. In this case, the satellite typically also indexes a cloud cover, and there is very little yield. Another possibility would be a frost cover after cold and humid nights. This state will change quickly after sunrise, resulting in only small losses. The reversed case, however, i.e., snow slipped off the module due to radiation and air temperature but the ground is still covered, will lead to an error at all events. Further assessment of these cases requests a separate snow-melting model for PV plants, which is out of the focus in this satellite-related study.

2.2. Quality metrics

Several quality metrics are defined for the comparison of satellite datasets against ground measurements. They use

different basic populations (N) and subsets (M) which are introduced as:

N_{total} = total number of cases
$N_{cloudless}$ = the cloudless cases indexed as either snow-covered or snow-free
N_{snow} = cases with snow cover indexed by the satellite
$N_{snowfree}$ = cases without snow cover indexed by the satellite
M_{csnow} = subset indexed correctly as snow cover
$M_{csnowfree}$ = subset indexed correctly as snow-free
M_{corr} = $M_{csnow} + M_{csnowfree}$
$M_{fsnowfree}$ = subset indexed falsely as snow-free
M_{fsnow} = subset indexed falsely as snow cover
M_{cloud} = subset indexed as cloudy

The quotient of the corresponding statements of ground and satellite (M_{corr}) over all cloudless values ($N_{cloudless}$) equals the classification accuracy (A_{class}):

$$A_{class} = \frac{M_{corr}}{N_{cloudless}} \times 100\% \quad (1)$$

Because of some datasets having the condition "cloudy", only those values with information on snow cover are used for the basic population. Days with no information on snow cover and indexed as cloudy are not taken into consideration. This is to assure that a correctly identified cloud will not be treated as an error in the dataset.

Section 2.1.3 (case B) discusses why the false alarm, an error based on snow which not indexed, is most problematic for plant management. To classify this error, a false alarm rate E_{alarm} is introduced as the quotient of pixels indexed as snow-free in spite of a snow cover over the basis N_{snow}.

$$E_{alarm} = \frac{M_{fsnowfree}}{N_{snow}} \times 100\% \quad (2)$$

This basic population is used to eliminate the dependency of E_{alarm} on the total amount of snow-covered days in the period under observation. Similar as discussed for A_{class}, only days without clouds are taken into consideration.

In the opposite case, an error due to underestimation E_{est} of solar irradiance and, therefore, energy yield (case D) describes cases with an indexed snow cover in spite of a snow-free ground.

$$E_{est} = \frac{M_{fsnow}}{N_{snowfree}} \times 100\% \quad (3)$$

The basic population consists of those values with a snow-free ground and no cloud cover indexed ($N_{snowfree}$). This ensures that E_{est} has no dependency on the total number of days without snow in datasets with different data availabilities.

To compare different algorithms, the availability A as percentage of days with information on snow cover is introduced. A has to be taken into consideration – together with the other quality metrics – to assess all datasets justly. Otherwise, datasets supplying information also on cloudy days would be discriminated in comparison with those datasets without such additional information on clouds.

$$A = 1 - \frac{M_{cloudy}}{N_{total}} \times 100\% \quad (4)$$

3. Data

3.1. Satellite data sources and snow algorithms

An overview on geographical coverage, spatial resolution, and possible pixel states for satellite data used in this study provides Table 2.

3.1.1. Automated snow mapping system (NOAA-STAR)

The algorithm operated by NOAA/NESDIS (National Oceanic and Atmospheric Administration/National Environmental Satellite, Data, and Information Service) for the GOES satellites (Romanov et al., 2003) was also ported to the Meteosat Second Generation (MSG) satellites. The main difference is that SEVIRI (Spinning Enhanced Visible and InfraRed Imager) channel 3 at 1.6 μm is taken instead of GOES channel 2 at 3.9 μm. To identify a snow-covered pixel, the algorithm takes all available daytime measurements in the 0.64 μm, 0.81 μm, 1.64 μm, and 10.8 μm channels into account. Additionally, a 'snow index' is defined as the ratio of the reflectances in the 0.64 and 1.64 μm channels. The final classification is made on the basis of fixed thresholds for brightness temperatures in the 10.8 μm channel, reflectances in the 0.6 and 1.6 μm channels and the snow index as described by Romanov and Tarpley (2005). This dataset provides values for each day by replacing missing data by previous classifications.

3.1.2. The Carl von Ossietzky University Oldenburg

The Carl von Ossietzky University Oldenburg supplies global irradiance data by using the Heliosat method (Hammer et al., 2003) for SEVIRI. The SAMSAT algorithm detecting snow cover situations has been introduced into Heliosat (Heinicke, 2006). A normalized differential snow index (NDSI), calculated from the difference of 0.6 and 1.6 μm channels divided by the sum of both channels, is applied to decide between snow and snow-free surfaces in clear-sky conditions. A NDSI < 0 indicates either a small cloud cover or a cloud- and snow-free land surface, while a NDSI > 0 results in additional threshold checks for the 12 μm brightness temperature and the 1.6 μm reflectance. If still no classification can be made due to ice clouds with similar characteristics than snow on the ground, further spectral differences are evaluated: Differences in the brightness temperatures of the 10.8 and the 3.9 μm channels between −10 K and +60 K indicate snow instead of ice clouds. This classification is finally supported if the brightness temperature difference in the 12.0 and 10.8 μm channels is in the range of 4.0 to 6.5 K. The SAMSAT based

Table 2
Overview of datasets compared in this study.

Provider	Satellite	Sensor	Resolution	Coverage	File type	Pixel states
Automated snow mapping system (NOAA-STAR)[a]	MSG	SEVIRI	4 km	25°N–65°N, 25°W–35°E (Europe)	Binary	No snow, land Snow Ice Cloud No classification
Carl von Ossietzky University Oldenburg[b]	MSG	SEVIRI	Data is provided for specified coordinates	Europe	CSV	No snow Snow Cloud
Carlo Gavazzi Space (CGS)[c]	Terra	MODIS	250 m	Alps: Northwest 48°11'/05°09' to Northeast 47°20'/06°39', Southwest 43°38'/05°27' to Southeast 43°37'/13°52'	Binary	No snow Snow Cloud No data
German Aerospace Center (DLR)[d]	MSG	SEVIRI	4 km @ Nadir	Europe, Northern Africa, Southern Africa, South America	HDF	No snow Snow Water No data Space
IMS NSIDC[e]	Aqua, Terra, MSG, POES	MODIS, SEVIRI, AVHRR, SSM/I, AMSU	4 km	Nordic Hemisphere	GeoTIFF ASCII	Land Snow Sea Ice Outside northern hemisphere
Land SAF (EUMETSAT)[f]	MSG	SEVIRI	4 km @ Nadir	Europe, Northern Africa, Southern Africa, South America	HDF 5	No snow Snow Not classified Partly snow-covered
MODIS (MOD10A1)[g]	Terra	MODIS	500 m	Worldwide	HDF EOS	No snow Snow Cloud Sea Lake Lake Ice Detector saturated Fill No decision Night

[a] http://www.orbit.nesdis.noaa.gov/smcd/emb/snow/HTML/europe_snow.html.
[b] http://www.energiemeteorologie.de/.
[c] http://www.cgspace.it/.
[d] http://wdc.dlr.de/.
[e] http://nsidc.org/data/g02156.html.
[f] http://landsaf.meteo.pt/.
[g] http://nsidc.org/data/mod10a1.html.

snow dataset is evaluated in this study. It contains missing values e.g. in cloudy situations. The dataset is experimental and covers the period from 1st January to 31st March 2006.

3.1.3. Carlo Gavazzi Space S.p.A. (CGS)

The dataset has been developed for hydropower plant management (Tampellini et al., 2007). It is based on MODIS reflectances with 250 m (MOD09GQK) and 500 m (MOD09GHK) ground resolution. Additionally, the snow cover map is corrected for errors introduced by coniferous forests by adding snow under coniferous trees depending on elevation. The coverage of the dataset is limited to the Alpine region. Gaps in the daily dataset are due to cloud cover. The dataset is experimental and covers the period from 1st January to 2nd March 2006.

3.1.4. German Aerospace Center (DLR)

The DLR algorithm is based on APOLLO developed originally for Advanced Very High Resolution Radiometer (AVHRR) data (Kriebel et al., 2003; Saunders and Kriebel, 1988), and ported to MSG SEVIRI. The SEVIRI version uses a dynamic snow threshold which is calculated from every scene separately. A snow index *sni* between 0 and 1 is calculated for each pixel as a sum of three criteria: Large reflectances above 0.45 in the 0.6 μm channel, small reflectances below 0.15 in the 1.6 μm channel, and 12.0 μm brightness temperatures close to 273 K contribute with a weight of 0.33, respectively. Reflectances between 0.15 and 0.45 in the 0.6 μm channel and reflectances between 0.15 and 0.45 in the 1.6 μm channel contribute with a weight varying linearly from 0 to 0.33 with the increase of 0.6 μm and the decrease of 1.6 μm reflectances. A similar linear weight modification

from 0.0 to 0.33 is applied for 12.0 μm brightness temperatures between 250 and 273 K (increasing weight) and 273 and 276 K (decreasing weight). The average sni_{mean} and the standard deviation sni_{sdev} of the snow index histogram are calculated for every MSG scene separately. The threshold value is set to $sni_{mean} + 0.5\ sni_{sdev}$. If the snow index exceeds this threshold, the pixel is indicated as snow-covered. Afterwards, temporal and spatial filters are applied following (Ruyter de Wildt et al., 2007) to fill gaps e.g. due to cloudy days and exclude single outliers. Finally, a daily snow cover product is derived without any missing values.

3.1.5. IMS NSIDC

NOAA/NESDIS started snow monitoring in 1966, since 2004 the product is available worldwide on a 4 km by 4 km grid. The analysts combine all NOAA satellites including geostationary satellites and microwave sensors in a semi-manual scheme and provide a classification for every day (Ramsey, 1998; Helfrich et al., 2007; NOAA/NESDIS/OSDPD/SSD, 2004). Visible imagery is primarily taken from AVHRR on NOAA/POES, MODIS on the EOS (Earth Observing System) Terra and Aqua satellites and geostationary satellites as GOES, GMS (Geostationary Meteorological Satellite) and MSG. In addition, ground weather observations and microwave products from the AMSU (Advanced Microwave Sounding Unit) on the EOS Aqua and Terra satellites and SSM/I from the DMSP (Defense Meteorological Satellite Program) satellites are incorporated. The microwave products, though at relatively low resolution, are used to get additional information on cloudy days. Also, snow products from NOHRSC are made available to the analyst as well as several automated snow detection layers developed by NESDIS and NCEP (National Centers for Environmental Prediction). Due to the combination of several data sources including radar satellites there are no missing values in this dataset.

3.1.6. LSA SAF (EUMETSAT)

LSA (Land Surface Analysis) SAF as a Satellite Application Facility of the European Organization for the Exploitation of Meteorological Satellites (EUMETSAT) provides a snow cover dataset based on a cloud mask created by the Nowcasting SAF on a daily bases using MSG data and a threshold based algorithm for reflectance and brightness temperatures rather similar to the APOLLO approach used by DLR (LSA SAF, 2008). The LSA SAF algorithm additionally performs spatial smoothing and a temporal integration of the previous 24 h satellite scenes to produce a daily composite snow cover map. Missing values occur due to cloud cover.

3.1.7. MODIS

The MODIS/Terra Snow Cover Daily L3 Global 500 m Grid (MOD10A1) dataset consists of 1200 km by 1200 km tiles of 500 m resolution data gridded in a sinusoidal map projection. To detect snow, the MODIS snow mapping algorithm employs a Normalized Difference Snow Index (NDSI) calculated as the difference of band 4 (0.55 μm) and band 6 (1.6 μm) divided by the sum of both channels and the reflectances in band 2 and 4 (Hall et al., 2002b, 2006; Klein et al., 1998). For the detection of snow in dense vegetation a criterion using NDSI and the normalized difference vegetation index (NDVI) is applied to pixels that have an NDSI value in the range of 0.1–0.4. Additionally, pixels with surface temperatures above 283 K are set to snow-free as a filter for bright warm surfaces erroneously detected as snow. Due to cloud cover, missing values occur in the daily datasets.

3.2. Meteorological ground station data for validation

Meteorological ground stations typically monitor snow depth. Fourteen stations in Southern Germany and 15 stations in Swiss regions attractive for PV systems, but with a typical annual snow cover, are used in this study (Table 3). Overall they are providing a total of 3300 measurements in the study period January to April 2006. The study period was selected as a very snowy winter case in Central Europe. The measurements in Germany are taken at 18:00 UTC, while Swiss stations report at 17:40 UTC. In both countries the measurement is done manually with an accuracy of ±1 cm (Ernst, 2008; Glatt, 2008).

Table 3
Locations of all meteorological ground stations in Germany and Switzerland.

Station	Longitude	Latitude
Switzerland		
Aigle	06° 55' E	46° 20' N
Altdorf	08° 38' E	46° 52' N
Basel-Binningen	07° 35' E	47° 32' N
Bern-Liebefeld	07° 25' E	46° 56' N
Buchs-Suhr	08° 04' E	47° 23' N
Chur-Ems	09° 32' E	46° 52' N
Fahy	06° 56' E	47° 25' N
Genève-Cointrin	06° 07' E	46° 15' N
Zürich	08° 34' E	47° 23' N
Lugano	08° 58' E	46° 00' N
Luzern	08° 18' E	47° 02' N
Magadino	08° 53' E	47° 00' N
Payerne	06° 57' E	46° 49' N
Sion	07° 20' E	46° 13' N
St. Gallen	09° 24' E	47° 26' N
Germany		
Weissenburg/Bay.	10° 58' E	49° 01' N
Nürnberg-Kra.	11° 03' E	49° 30' N
Straubing	12° 34' E	48° 50' N
Augsburg-Mühlheim	10° 57' E	48° 26' N
Landsberg	10° 54' E	48° 04' N
Ingolstadt	11° 32' E	48° 43' N
München Stadt	11° 33' E	48° 10' N
Fürstenzell	13° 21' E	48° 33' N
Konstanz	09° 11' E	47° 41' N
Oberstdorf	10° 17' E	47° 24' N
Altenstadt	10° 52' E	47° 50' N
Hohenpeissenberg	11° 01' E	47° 48' N
Garmisch-Partenkirchen	11° 04' E	47° 29' N
Wendelstein	12° 33' E	47° 53' N

4. Results

It has to be noted, that some datasets provide daily information without any missing values while other datasets provide only snow maps for cloud free pixels and sufficient satellite viewing geometry and consequently, include gaps on several days. In a first approach, daily values as provided by the different data centers are compared to ground measurements for all days with non-missing values (Section 4.1). This results in a different number of days for each data set in the study period. In a second approach (Section 4.2), daily values at cloud-free days are compared to exclude differences due to different cloud detection schemes and to provide an answer to solar energy users for those days with high energy yields and a higher risk of a false alarm in the plant monitoring. In a third approach (Section 4.3), a cumulative gap filling algorithm based on (Ruyter de Wildt et al., 2007) is applied to derive daily snow cover time series without any gaps. The latter is also of practical importance for solar energy users as photovoltaic systems operate also in partly cloudy or low cloud optical depth conditions when satellite-based snow detection is already impossible.

4.1. Daily values without any gap filling algorithm

All statistics are calculated once for the whole dataset and also separately for Germany and Switzerland to take Alpine conditions into account. The LSA SAF dataset achieves the highest overall A_{class} with 76% (Fig. 1), while the datasets of DLR and Carlo Gavazzi Space reach 70%. LSA SAF and DLR use temporal and spatial information of the frequent Meteosat scenes, while the CGS dataset has advantages because of the high resolution of MODIS and specific adaptations to the Alpine region for hydropower management. This leads to the good classification in Switzerland. Global products as IMS (72%), NOAA-STAR (78%) and MODIS (79%) as well as the product from the University of Oldenburg show good classification accuracies with over 70% in Germany with its more homogenously structured land, whereas the classification in Switzerland drops to 49% (IMS) or 53% (Univ. Oldenburg) mainly as a result of the topography.

The IMS product uses additional microwave sensors providing information even on cloudy days. On the other hand, these sensors have a spatial resolution of typically 100–200 km^2 which is much smaller compared to a few km^2 in the visible and infrared range used by other algorithms. This leads to quantification errors and the product looses overall quality compared to the cloud-free only algorithms.

E_{alarm} gives a different view, as the lowest false alarm rate is achieved by IMS with 4%. Fig. 2 illustrates E_{alarm} as rising bars from the zero line and E_{est} as bars descending from that line. Both errors combined are a measure for the total error, but it has to be taken into consideration that a different basic population is applied. E_{alarm} refers to the

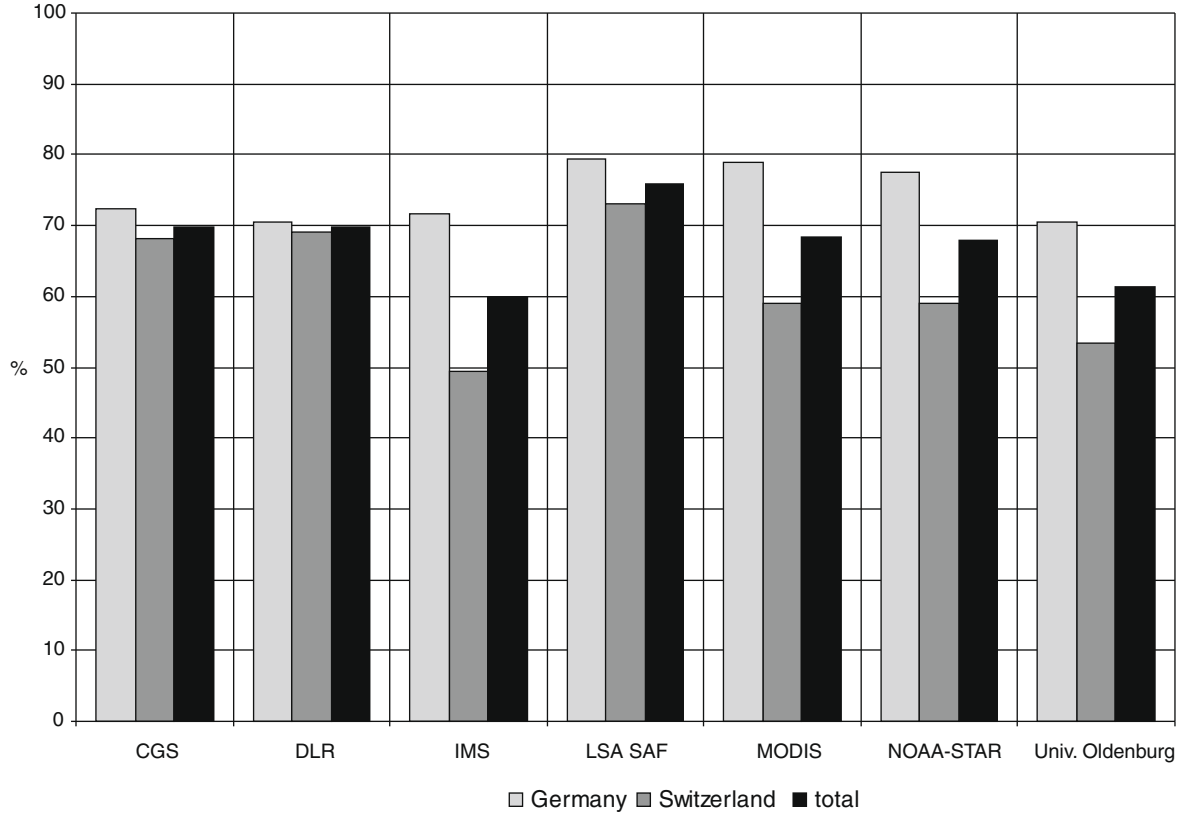

Fig. 1. Relative classification accuracy of all datasets versus SYNOP ground observations in January to April 2006 for Germany and Switzerland.

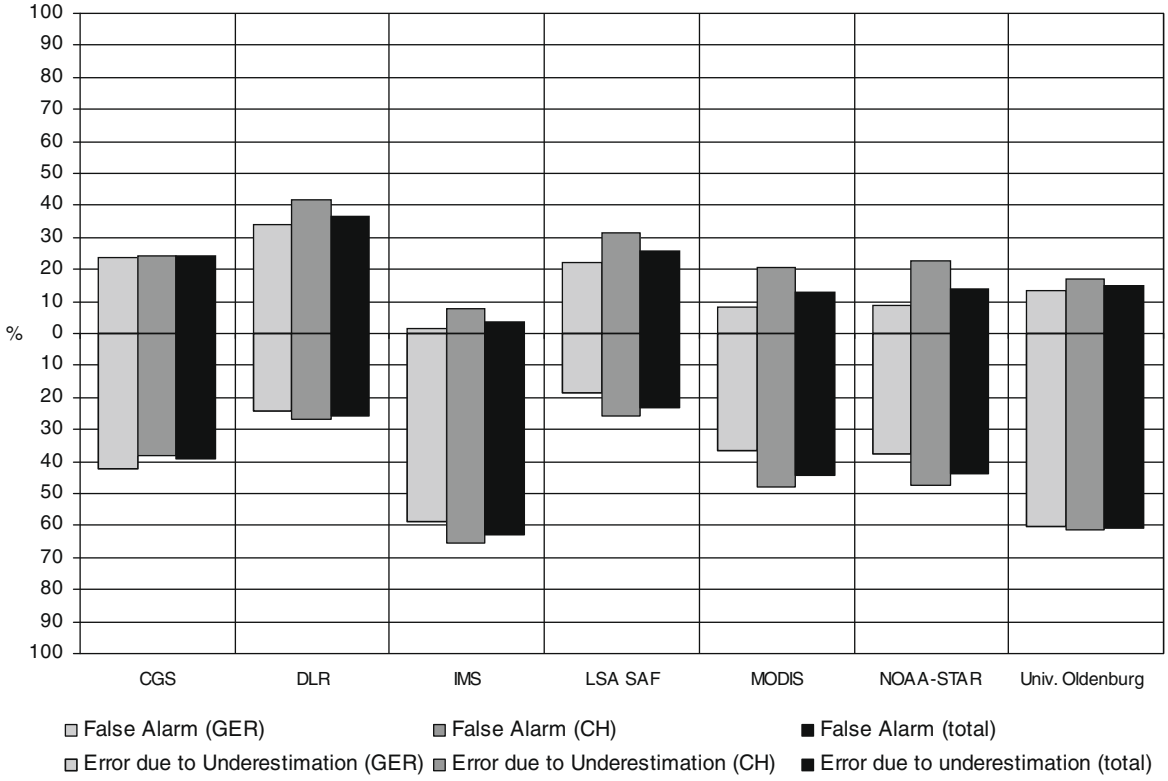

Fig. 2. False alarm rates (snow cover not detected by satellites) and the error due to radiance underestimation (too much snow cover detected by satellites) of all datasets versus SYNOP ground observations in January to April 2006 for Germany and Switzerland.

days with a snow-covered ground whereas E_{est} is based on the days without snow.

Fig. 2 demonstrates different strategies of the respective algorithms. The error shifts from an overestimation to an underestimation of indicated snow, depending upon how defensively snow detection is handled. The IMS dataset combines a small E_{alarm} with a high E_{est} (63%), whereas the LSA SAF dataset has the most symmetrical error pattern (26 to 23%). Both, DLR and CGS also have a well balanced error pattern (37 to 26% and 24 to 39%, respectively), while the patterns of the NOAA-STAR (14 to 44%) and the University of Oldenburg (15 to 61%) datasets are clearly shifted towards E_{est}.

For all these analyses, A has to be considered as an additional criterion (Fig. 3). While IMS and NOAA-STAR state a value every day, the MODIS dataset delivers a value only on 29% of the days in the study period. This exhibits the disadvantage of the MODIS spectrometer which is mounted on a low-orbiting satellite and passes a spot only once a day. If the sky is cloudy at that time, no classification can be made. NOAA-STAR, LSA SAF and the University of Oldenburg datasets have a much higher probability of matching a cloudless window due to the 15 min sample rate of MSG.

Differences in A between datasets using the same sensors depend on the parameters of the respective algorithm. Some datasets use information of preceding days as an additional input parameter. The selection of thresholds for the discrimination of snow also leaves its footprint in this analysis. The product of the University of Oldenburg uses the same input values as the LSA SAF product but gets a higher A (81%) because it classifies snow as soon as one slot is indicated as snow-covered. The LSA SAF product ($A = 65\%$) requests a reasonable majority of slots to be detected as snow, otherwise the pixel will be set to unclassified. Secondly, the DLR product reaches almost $A = 100\%$ because it is based on a cumulative gap filling approach.

4.2. Daily values in clear-sky cases only

In practice, it is especially relevant how a dataset performs in clear-sky conditions, as these days have the maximum power output, and errors have the largest impact on the economics of a solar power plant. Algorithms providing cloudy case information also had a disadvantage in the first comparison strategy, as it is expected that satellite retrieval performance is reduced in cloudy cases. This is eliminated in the following comparison.

In order to avoid errors in snow-cloud discrimination in the satellite information, meteorological ground stations are taken as ground truth for cloud coverage. This record is expressed in octa, values below two octa are taken as the threshold to determine a cloudless sky. It has to be noted that the cloud cover record from ground measurements was available for this study only in Germany. Additionally, clear-sky days were rare in the validation period, and so the statistical basis of the analysis is significantly

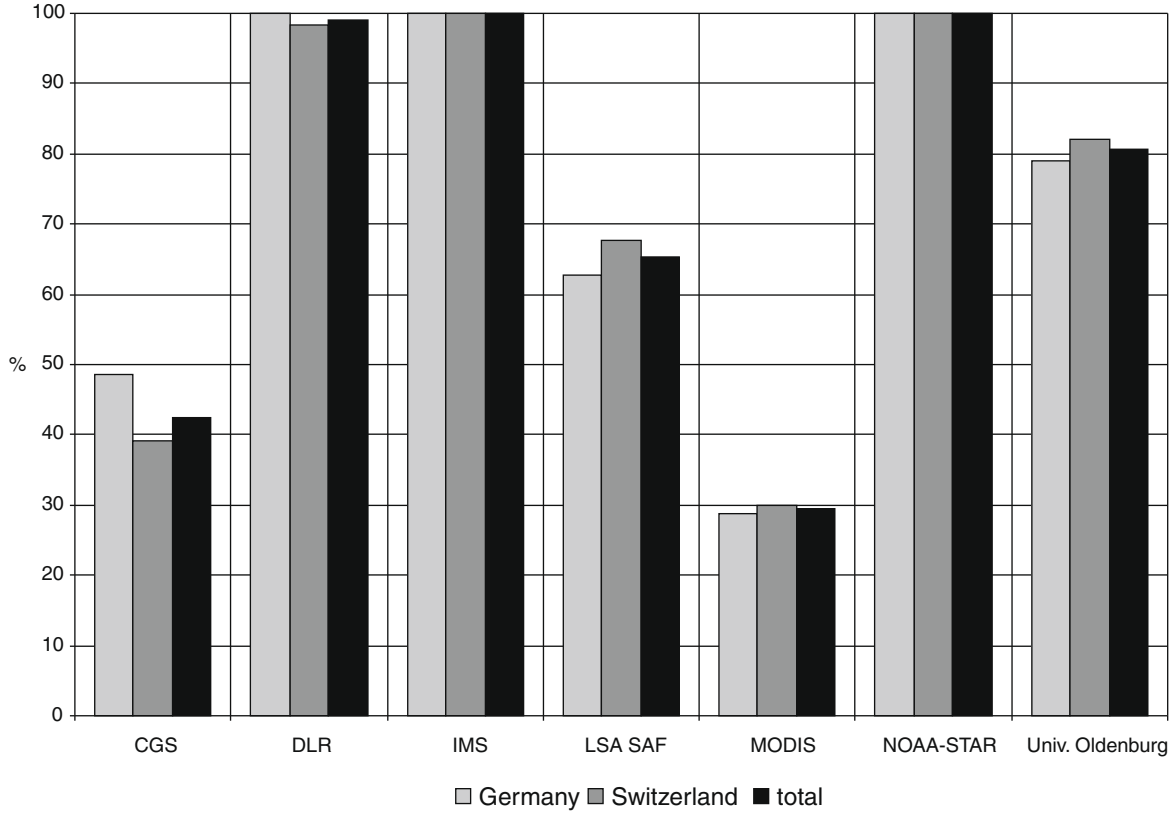

Fig. 3. Percental availability of daily values in different data sources in the period January to April 2006 for Germany, Switzerland and both regions together.

reduced from 3300 to only 150 ground measurements. Coincidences for the CGS dataset are even reduced to 60 values because not all the German stations are covered by this dataset. Therefore, the analysis serves more to verify whether the existing methods are suitable for clear-sky days and whether there are significant performance differences in clear-sky cases compared with all sky cases.

The results correspond with the results presented in Section 4.1. A_{class} increases slightly by 2 to 7%, the dataset of the University of Oldenburg even by 13%. This result is anticipated because the classification on clear-sky days is more reliable than in cloudy conditions. A_{class} of the MODIS dataset, however, decreases by 3% due to a high E_{est}.

E_{alarm} stays equal (IMS) or is decreasing with all the datasets (NOAA-STAR −8%, LSA SAF −17%, Univ. Oldenburg −5%, DLR −15%, MODIS −5%), corresponding with higher A_{class}. With 26%, only the CGS dataset shows a slightly higher E_{alarm}, but due to the small basic population this can be insignificant.

In the opposite case, E_{est} behaves not as homogenously as A_{class} and E_{alarm}. Most datasets show a decline, CGS even to 0%. The products of LSA SAF (+5%), MODIS (+14%), and the DLR (+6%) show an increase in contrast to the other datasets (IMS −3%, NOAA-STAR −2%, Univ. Oldenburg −26%). This indicates that cloud and snow confusion reduces the performance in clear-sky days for LSA SAF, MODIS, and DLR datasets, which could indicate that these datasets have problems distinguishing between ice clouds and snow.

4.3. Daily values using a cumulative gap filling algorithm

For plant management, it is beneficial to have a classification every day even if the snow detection algorithm fails due to satellite viewing or cloud conditions. A cumulative algorithm – for example Ruyter de Wildt et al. (2007) as used in the DLR dataset – can provide this interpolation. Basically, a cumulative algorithm keeps the snow cover information of one day at a pixel until a new classification is received. As a result, even on days with missing values snow cover information can be supplied relying on preceding days.

Obviously, such an interpolation causes a decrease of A_{class} for those datasets delivered by the provider with gaps due to cloud cover (CGS +12%, LSA SAF +6%, University of Oldenburg +2%, and MODIS +9%) as shown in Fig. 4. A higher A is also linked to a degradation of the error values (Fig. 5). E_{alarm} increases (CGS +6%, LSA SAF +9%, University of Oldenburg +2%, and MODIS +16%) as well as E_{est} (CGS +15%, LSA SAF +4%, University of Oldenburg +4%, and MODIS +2%).

Despite this decrease in the performance of the datasets, this approach is useful in practice because it results in information being available every day. It should be noted

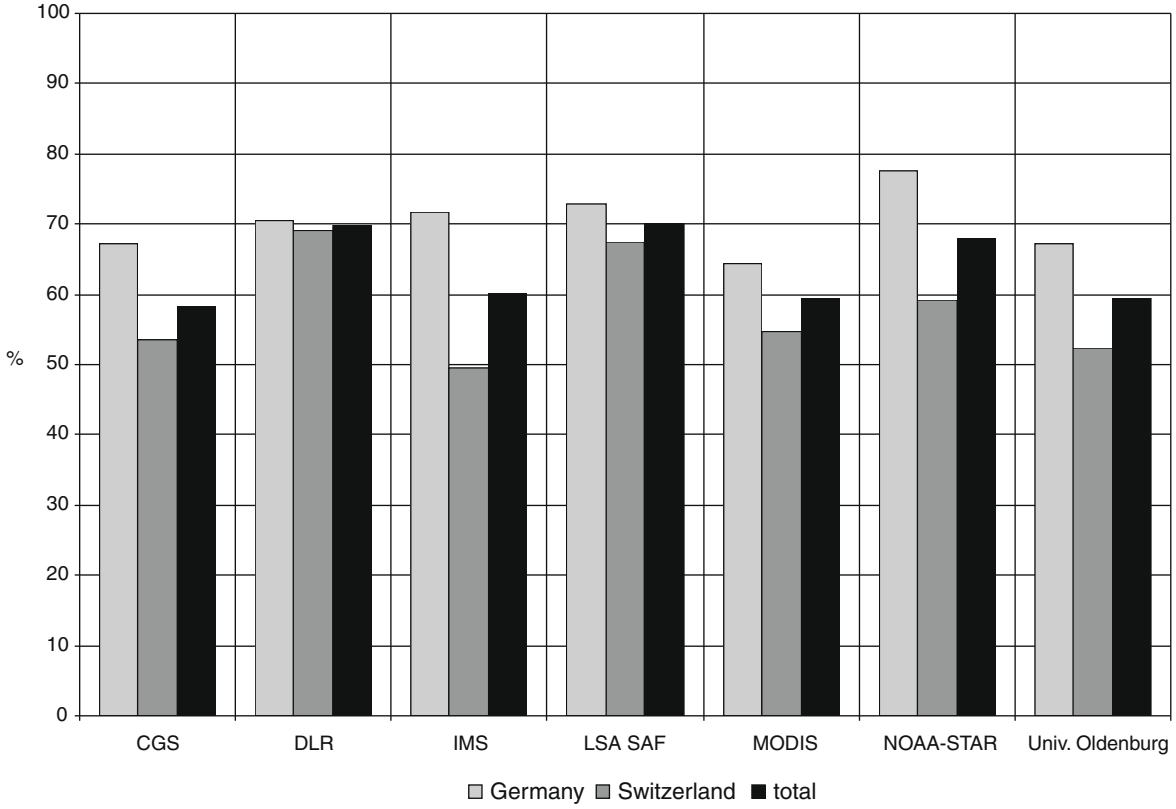

Fig. 4. Relative classification accuracy for a cumulative data post-processing approach filling missing days by information from previous days with existing measurements. Comparison results versus SYNOP ground observations for January to April 2006 in Germany and Switzerland are presented separately and summed up for both regions.

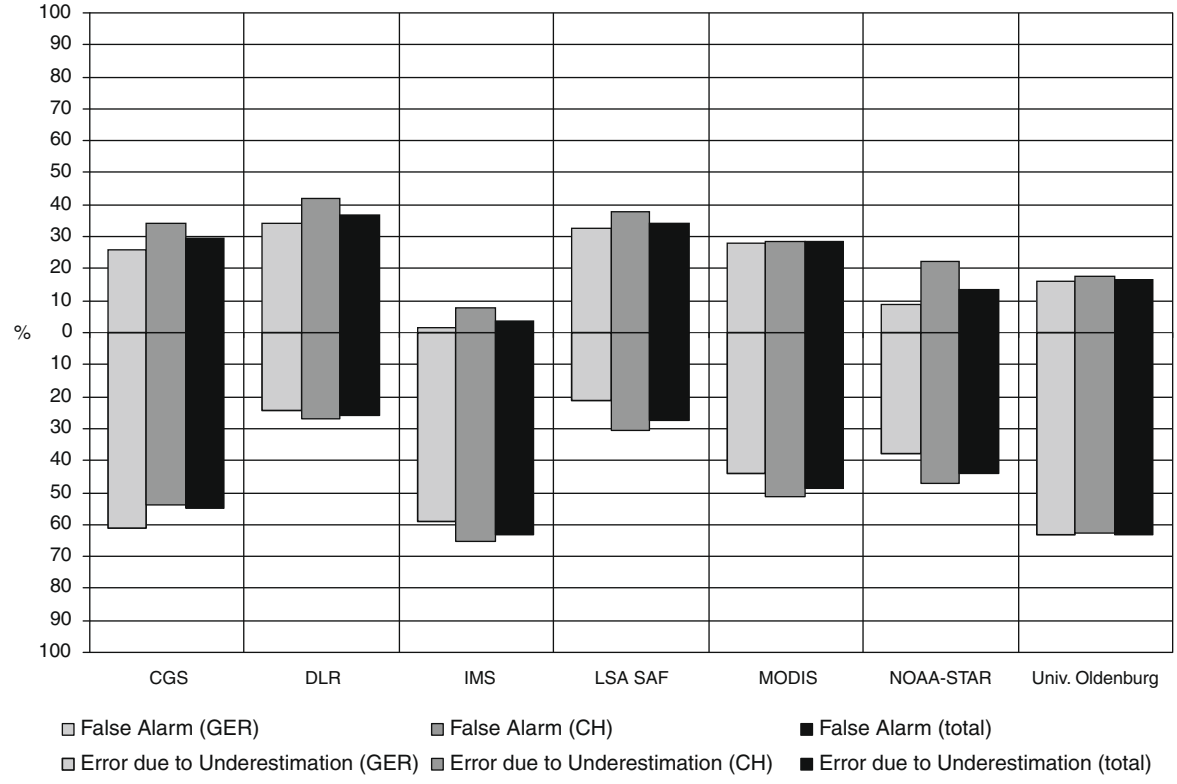

Fig. 5. False alarm rates (snow cover not detected by satellites) and the error due to radiance underestimation (too much snow cover detected by satellites) of all daily datasets completed with a cumulative post-processing approach versus SYNOP ground observations in January to April 2006 for Germany and Switzerland.

that this approach leads to a leveling of the leading position of the LSA SAF dataset compared with the DLR dataset in the validation.

5. Conclusion and discussion

There are two main objectives for the use of satellite-based snow observations in the management of photovoltaic systems. Avoiding a false alarm is of high importance for any PV plant monitoring system. Therefore, every day with snow cover needs to be identified correctly. By now, snow data is used as additional information in a plant monitoring system to enable the operator to judge if an already detected plant failure is based on snow cover only. In such cases the raised alarm can be rejected avoiding useless maintenance and repair efforts, e.g. at remote solar installations. The error due to irradiance underestimation is less critical for plant monitoring as it represents only indicated snow in snow-free situations. Such a situation will not create a false alarm, but reduce the system's sensitivity for faults and might therefore miss a true alarm.

Yield estimation for site auditing and investment calculations, on the other hand, has a demand for a symmetrical and small total error in order to achieve a high classification accuracy together with a low overall bias. For yield estimates average snow cover days calculated from historical databases supply additional information on the typical losses due to snow at a specific location.

Finally, snow cover could be used in the calculation of global irradiance directly, e.g. by replacing a cloud index representing a cloudy case by a typical cloud free value in case of a satellite-retrieved cloud cover.

Several satellite-based datasets are compared against 29 meteorological ground stations in Southern Germany and Switzerland for the period January to April 2006. The results of the different datasets vary depending on the analyzed region and the intended application in solar energy. A clear difference between Southern Germany and Switzerland is recognizable especially for those datasets with lower pixel resolution as mixed pixels due to snow at high altitudes and snow-free valleys are more frequent in the Alpine regions.

The classification accuracy is defined as the agreement of satellite and ground measurements both in snow and snow-free cases. A false alarm rate is defined as the quotient of pixels retrieved as snow-free in spite of a snow cover in coincident ground measurements. In the opposite case, the error due to underestimation of energy yield shows the values with a retrieved snow cover in spite of a snow-free ground.

First, all datasets are assessed taking all non-missing values into account. Generally, classification accuracy above 70% is achieved in Germany with a maximum of 79% for the LSA SAF dataset. In Switzerland, the datasets of IMS, NOAA-STAR, MODIS, and the University of Oldenburg show less than 60% classification accuracy.

The LSA SAF dataset has a symmetrical and small error pattern (false alarm rate 26%, error due to underestimation 23%), but the data availability is low (65%). Also, the DLR dataset has a rather small symmetrical error pattern (false alarm rate 37%, error due to underestimation 26%) and a good availability (99%).

The IMS dataset shows a low false alarm rate (4%, 1% in Germany, 8% in Switzerland) and good data availability (100%), but a large error due to underestimation (59%). It is therefore well suited for the purpose of avoiding false alarms in power plant monitoring due to existing snow cover, but can not be recommended for site auditing.

For all these characteristics, the availability of each dataset has to be considered for a complete view. Missing values are typically due to cloud cover or the satellite viewing geometry. DLR, NOAA-STAR, and IMS supply an every-day value, whereas the MODIS product contains only information on 29%, CGS on 42%, LSA SAF on 65%, and University of Oldenburg on 81% of all days in the validation period.

An analysis of cloudless days only – as the days with highest energy yields – confirms the results obtained for all sky conditions.

Finally, a cumulative algorithm is applied to fill gaps in all datasets. Such an approach is needed for those users requesting information on every day. Generally, this increase in information is coupled with a reduction in classification accuracy. Both, the DLR and LSA SAF datasets show the best and also comparable results in A_{class} (DLR 70%, LSA SAF 70%), in the false alarm rate (DLR 37%, LSA SAF 34%) and in the error due to underestimation (DLR 26%, LSA SAF 27%).

Overall, both LSA SAF and DLR datasets are best suited if all solar energy purposes are taken into account. They provide a symmetric error pattern together with the best classification accuracy. The IMS dataset shows a lower overall accuracy, but also the lowest false alarm rate which makes it most suitable if the user is interested only in avoiding false alarms in a plant monitoring scheme and can accept a strong overestimation of snow cover.

The next step to increase snow detection accuracy in PV plant monitoring could be the coupling with a snow-melting model describing how snow melts off the panel, leaving it only partly covered. Nevertheless, for the main objective of reducing cases of false alarm involving costly and inefficient maintenance staff assignment, this additional case of snow on the ground but not on the panel resulting in an overassessed power yield is of minor relevance.

Acknowledgements

We thank the National Snow and Ice Data Center of the National Oceanic and Atmospheric Administration (NOAA) for providing the MODIS and IMS data, Dr. Peter Romanov for the NOAA-STAR dataset, and the Land Surface Analysis Satellite Applications Facility for the LSA SAF dataset. We, furthermore, express our special gratitude to the Carl von Ossietzky University Oldenburg, Carlo Gavazzi Space S.p.A. (CGS), and the ICSU World

Data Center for Remote Sensing of the Atmosphere (WDC-RSAT) operated at DLR, who created their data sets for this study specifically.

References

Basist, A.B., Garrett, D., Ferraro, R.F., Grody, N., Mitchell, K., 1996. A comparison between snow cover products derived from visible and microwave satellite observation. Journal of Applied Meteorology 35 (2), 163–177.

Bitner, D., Carroll, T., Cline, D., Romanov, P., 2002. An assessment of the differences between three satellite snow cover mapping techniques. Hydrological Processes 16 (18), 3723–3733.

Brubaker, K., Pinker, R., Deviatova, E., 2005. Evaluation and comparison of MODIS and IMS snow-cover estimates for the continental United States using station data. Journal of Hydrometeorology 6 (6), 1002–1017.

Drews, A., de Keizer, A.C., Beyer, H.G., Lorenz, E., Betcke, J., van Sark, W.G.J.H.M., Heydenreich, W., Wiemken, E., Stettler, S., Toggweiler, P., Bofinger, S., Schneider, M., Heilscher, G., Heinemann, D., 2007. Monitoring and remote failure detection of grid-connected PV systems based on satellite observations. Solar Energy 81, 548–564.

Ernst, W., 2008. Personal communication based on metadata information available at DWD.

Glatt, P., 2008. Personal communication based on metadata information available at MeteoSchweiz.

Hall, D.K., Foster, J.L., Verbyla, D.L., Klein, A.G., Benson, C.S., 1998. Assessment of snow cover mapping accuracy in a variety of vegetation cover densities in central Alaska. Remote Sensing of the Environment 66, 129–137.

Hall, D.K., Kelly, R.E.J., Riggs, G.A., Chang, A.T.C., Foster, J.L., 2002a. Assessment of the relative accuracy of hemispheric-scale snow-cover maps. Annals of Glaciology 34, 24–30.

Hall, D.K., Salomonson, V.V., Riggs, G.A., DiGirolamo, N., Bayr, K.J., 2002b. MODIS snow cover products. Remote Sensing of Environment 83, 181–194.

Hall, D.K., Solberg, R., Casey, K.A., Winther, J.G., 2004. Comparison of MODIS and SnowStar Maps in Scandinavia. In: Proceedings of the 61st Eastern Snow Conference, 9–11 June 2004, Portland, ME,USA. pp. 75–80.

Hall, D.K., Riggs, G.A., Salomonson, V.V., 2006. Updated Daily, MODIS/Terra Snow Cover Daily L3 Global 500 m Grid V005, January Through April 2006. National Snow and Ice Data Center, Digital Media, Boulder, Colorado USA.

Hammer, A., Heinemann, D., Hoyer, C., Kuhlemann, R., Lorenz, E., Müller, R., Beyer, H.G., 2003. Solar energy assessment using remote sensing technologies. Remote Sensing of Environment 86, 423–432.

Heinicke, S., 2006. Schneeerkennung auf Basis von multispektralen und multitemporalen Meteosat-8-Informationen–Einbettung in das bestehende Verfahren der HELIOSAT-Methode, Diplomarbeit. Fachbereich Physik, Carl von Ossietzky-Universität, Oldenburg.

Helfrich, S.R., McNamara, D., Ramsay, B.H., Baldwin, T., Kasheta, T., 2007. Enhancements to and forthcoming developments to the Interactive Multisensor Snow and Ice Mapping System (IMS). Hydrological Processes 21 (12), 1576–1586.

Klein, A.G., Hall, D.K., Riggs, G.A., 1998. Improving snow cover mapping in forests through the use of a canopy reflectance model. Hydrological Processes 12, 1723–1744.

Kriebel, K.T., Gesell, G., Kästner, M., Mannstein, H., 2003. The cloud analysis tool APOLLO: Improvements and Validation. International Journal of Remote Sensing 24, 2389–2408.

LSA SAF, 2008. SC Product User Manual, Ref. SAF/LAND/FMI/PUM/SC/2.8, Version 2.8, 10 October 2008.

Maurer, E., Rhoads, J., Dubayah, R., Lettenmaier, D., 2003. Evaluation of the snow-covered area data product from MODIS. Hydrological Processes 17, 59–71.

NOAA/NESDIS/OSDPD/SSD, 2004. Updated 2006. IMS daily Northern Hemisphere snow and ice analysis at 4 km and 24 km resolution. National Snow and Ice Data Center, Digital media, Boulder, CO.

Ramsey, B.H., 1998. The interactive multisensor snow and ice mapping system. Hydrological Processes 12, 1537–1546.

Romanov, P., Tarpley, D., Gutman, G., Carroll, T., 2003. Mapping and monitoring of snow cover fraction over North America, Journal of Geophysical Research 108, 8619. doi:10.1029/2002JD003142.

Romanov, P., Tarpley, D., 2005. Monitoring snow cover over Europe with Meteosat SEVERI. Proceedings of the 2005 EUMETSAT Meteorological Satellite Conference. 19–23 September 2005, Dubrovnik, Croatia (EUMETSAT P.46).

Romanov, P., Gutman, G., Csiszar, I., 2000. Automated monitoring of snow cover over North America with multispectral satellite data. Journal of Applied Meteorology 39, 1866–1880.

Ruyter de Wildt, M., Seiz, G., Gruen, A., 2007. Operational snow mapping using multitemporal Meteosat SEVIRI imagery. Remote Sensing of Environment. 109, 29–41.

Saunders, R.W., Kriebel, K.T., 1988. An improved method for detecting clear sky and cloudy radiances from AVHRR data. International Journal of Remote Sensing 9, 123–150.

Simic, A., Fernandes, R., Brown, R., Romanov, P., Park, W., 2004. Validation of VEGETATION, MODIS, and GOES + SSM/I snow-cover products over Canada based on surface snow depth observations. Hydrological Processes 18, 1089–1104.

Tampellini, L., Ober, G., Vescovi, F.D., Power, D., Strozzi, T., Vincent, P., Eikvil, L., Malnes, E., Nagler, T., Rott, H., 2007. EO-hydro an earth observation service for hydropower plant management. In: Proceedings of the ENVISAT Symposium, 23–27 April 2007. Montreux, Switzerland.